Civil Engineering and Applied Solutions

Research Article

journal homepage: ceas.journals.umz.ac.ir

CEAS Civil Engineering and Applied Solutions

Earthquake-Induced Deformation of Road Embankments: A Finite Difference Method

Vahid Sadeghi [a], Mohsen Bagheri [b*], Jaber Abasi Hamidi [a]

[a] *Department of Civil Engineering, Saroyeh Institute of Education, Sari, Iran*
[b] *Faculty of Civil Engineering, Babol Noshirvani University of Technology, Babol, Iran*

ARTICLE INFO

Keywords:
Road embankments
Seismic performance
Dynamic numerical analysis
Soil liquefaction
FLAC

Article history:
Received 15 December 2025
Accepted 23 April 2026
Available online 01 October 2026

ABSTRACT

This paper presents a numerical study on the seismic performance of road embankments using finite difference modeling implemented in FLAC. Nonlinear dynamic analyses are conducted to quantify the effects of critical seismic parameters, including peak ground acceleration (PGA) and thickness of liquefiable soil on deformation patterns and settlement behavior of embankments. The results demonstrate that elevated groundwater conditions and the onset of soil liquefaction markedly intensify permanent deformations and compromise global stability. Maximum displacements are predominantly generated during the strong-motion phase of the earthquake, followed by a degree of post-shaking stabilization that is strongly governed by soil mechanical properties. The induced deformations may lead to longitudinal and transverse cracking, reduction in effective embankment height, and progressive modification of slope geometry, thereby impairing structural integrity and traffic safety. The study highlights the importance of incorporating seismic frequency content, coupled hydro-geotechnical conditions, and soil strength characteristics into the seismic design, evaluation, and rehabilitation of road embankments in earthquake-prone areas. The findings contribute to improving predictive assessments and offer practical implications for enhancing the seismic resilience of transportation infrastructure.

1. Introduction

Iran is situated within the Alpine–Himalayan seismic belt, one of the most tectonically active regions in the world, and is therefore repeatedly subjected to moderate to strong earthquakes. Numerous historical and recent seismic events have resulted in extensive damage to transportation infrastructure, particularly road embankments, which constitute a fundamental component of road networks. The seismic vulnerability of these earth structures poses a serious challenge, as their failure can severely impair traffic circulation, delay emergency operations, and hinder post-earthquake recovery.

Road embankments are commonly constructed to overcome complex topographical conditions, provide grade separation, and ensure continuity of transportation corridors. Under seismic loading, however, these structures are exposed to inertial forces, cyclic shear stresses, and excess pore water pressure generation, which may lead to large permanent deformations, slope instability, and in severe cases, liquefaction-induced failure. Previous studies have shown that earthquake-induced damage to embankments can cause disruptions comparable to, or even exceeding, those observed in structural roadway elements such as bridges and pavements, particularly when constructed on soft or saturated soils [1, 2]. Field evidence from major earthquakes, including the Bam (2003), East Azerbaijan (2012), and Kermanshah (2017) events, has highlighted the susceptibility of Iranian road embankments to seismic loading. In many cases, embankments are founded on weak or fine-grained soils with high plasticity, especially along rural and

* Corresponding author.
E-mail addresses: m.bagheri@stu.nit.ac.ir (M. Bagheri).

https://doi.org/10.22080/ceas.2026.30800.1066
ISSN: 3092-7749/
How to cite this article: Sadeghi, V., Bagheri, M., Abasi Hamidi, H. Earthquake-Induced Deformation of Road Embankments: A Finite Difference Method. Civil Engineering and Applied Solutions. 2026; 2(4): 28–41. doi:10.22080/ceas.2026.30800.1066.

secondary road networks where locally available materials are widely used. Although these soils may perform adequately under static conditions, their stiffness and shear strength can degrade significantly during seismic shaking, resulting in excessive settlement, cracking, and loss of stability. The challenge of improving embankment performance in seismic regions is further compounded by economic, environmental, and geographical constraints. Large-scale replacement of weak soils or extensive structural interventions are often impractical. Consequently, there is a growing need for efficient and sustainable solutions that enhance the dynamic behavior of embankments while minimizing construction costs and environmental impacts. Soil stabilization and reinforcement techniques, including chemical additives, geosynthetics, and innovative eco-friendly materials, have emerged as promising approaches to mitigate seismic-induced deformations and improve overall stability. Despite existing research, there remains a need for comprehensive numerical investigations that explicitly account for dynamic loading characteristics, groundwater conditions, and soil improvement measures within a unified framework. In this study, the seismic response of road embankments under dry and saturated conditions is examined through advanced finite difference modeling using FLAC. The primary objective is to evaluate the effectiveness of selected stabilization strategies in reducing permanent deformations and enhancing embankment resilience under earthquake loading. The outcomes of this research aim to provide practical insights and design-oriented guidance for improving the seismic performance of road embankments, thereby contributing to the resilience and sustainability of transportation infrastructure in earthquake-prone regions.

2. Literature review

Earthquake-induced permanent deformations in road embankments are commonly attributed to several fundamental mechanisms, which may act independently or simultaneously depending on the soil conditions and seismic characteristics. These mechanisms can be broadly classified into compaction, lateral spreading, and global instability, as schematically illustrated in Fig. 1. Each mechanism reflects a distinct mode of soil response and deformation pattern under cyclic loading. Global instability is typically associated with the localization of shear and deviatoric strains along a well-defined failure surface, leading to large-scale slope failure or rotational sliding. In contrast, compaction and lateral spreading are characterized by more diffuse deformation processes. Compaction involves volumetric strain accumulation caused by cyclic densification of loose soils, whereas lateral spreading results from plastic shear deformations that develop over a wider zone, often triggered or amplified by excess pore water pressure generation. These mechanisms lead to progressive settlement, horizontal displacement, and gradual alteration of the embankment geometry rather than abrupt collapse. A clear distinction between these deformation modes is essential for accurate seismic performance evaluation and for the development of effective mitigation and retrofitting strategies. Failure to identify the dominant mechanism may result in inadequate design solutions or underestimation of seismic risk. Post-earthquake reconnaissance studies and documented case histories provide valuable insights into these behaviors. Representative examples of road embankment failures observed during various seismic events are presented in Figs. 2–7 [3, 4], illustrating the range of damage severity and the influence of local soil conditions, groundwater levels, and earthquake characteristics. Previous studies have emphasized that the interaction between seismic loading parameters and site-specific geotechnical conditions governs the dominant deformation mechanism and the resulting embankment response. Consequently, advanced numerical modeling and well-calibrated analytical approaches are increasingly employed to capture these complex behaviors and to improve the reliability of seismic assessment methods for road embankments.

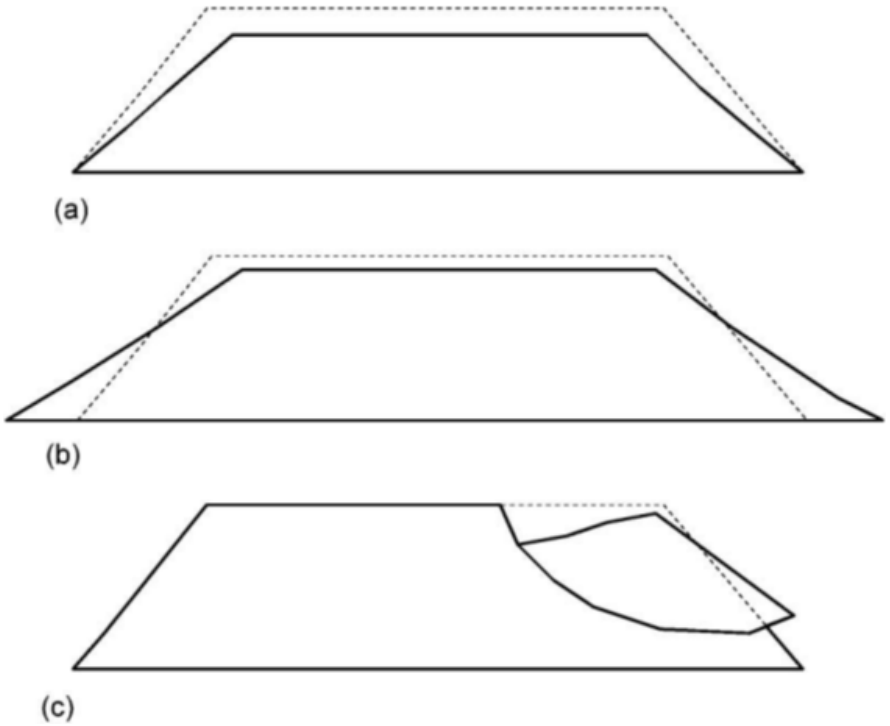

Fig. 1. Conceptual illustration of permanent deformation mechanisms in road embankments subjected to seismic loading: (a) volumetric compaction, (b) lateral spreading, and (c) global slope instability. Dashed outlines represent the initial (undeformed) configuration, while solid outlines indicate the post-earthquake deformed geometry.

Fig. 2. Vertical cracking observed along road alignments following the Haiti earthquake.

Fig. 3. Permanent embankment displacements near an overpass caused by the 1980 Irpinia earthquake, Lioni, Italy.

Fig. 4. Surface cracking on a road embankment after the 1980 Irpinia earthquake, Lioni, Italy.

Fig. 5. Vertical cracking in a road embankment during the Haiti earthquake.

Fig. 6. Shear failure in a road embankment during the 2010 Chile earthquake, showing notable lateral pavement displacement.

Fig. 7. Longitudinal cracking in a road embankment during the Peru earthquake, reflecting tensile stresses along the road axis.

In recent years, extensive numerical research has been devoted to improving the understanding of the seismic behavior of road embankments, particularly in regions characterized by high seismicity and soils prone to liquefaction. Strong ground motions can induce significant degradation of soil shear strength, generate excess pore water pressures, and result in large permanent settlements and lateral displacements. These complex soil–structure interactions highlight the necessity for reliable seismic performance assessment frameworks and resilient design methodologies for transportation infrastructure.

Khalil et al. [5] developed numerical fragility curves for highway embankments using a multi-mechanism elasto-plastic constitutive formulation. In their study, embankment settlement was adopted as the damage variable, while peak ground acceleration (PGA) served as the intensity measure, enabling a probabilistic evaluation of seismic vulnerability. Similarly, Oblak et al. [6] employed the advanced PM4Sand constitutive model to simulate liquefaction-induced deformations, using permanent settlement at the embankment crest as a damage index. Their results demonstrated that the use of state-of-the-art constitutive models significantly enhances the accuracy of predicting embankment response under earthquake loading, particularly in liquefiable soil conditions.

Further investigations have focused on the performance of the UBC3D-PLM model in capturing the dynamic response of embankments subjected to seismic excitation. Studies by Chakraborty and Sawant [7] confirmed the capability of this constitutive model to realistically reproduce key mechanisms such as dilation, cyclic mobility, and permanent deformation in sandy and silty deposits. These findings underscore the robustness of UBC3D-PLM as an effective numerical tool for simulating complex soil behavior and evaluating embankment performance in earthquake-prone environments.

At the network level, one of the most comprehensive efforts to date is the REDARS 2 framework, developed through a collaborative initiative between the Multidisciplinary Center for Earthquake Engineering Research (MCEER) and the Federal Highway Administration (FHWA). Introduced in 2006, REDARS 2 provides a systematic methodology and software platform for seismic risk assessment of highway systems. The framework integrates regional seismic hazard analysis, component-level damage modeling for bridges, roadways, tunnels, and embankments, and traffic network simulation to quantify post-earthquake disruptions. While REDARS 2 has been primarily calibrated for regions such as California, its development highlighted the critical need for region-specific seismic risk assessment tools that reflect local geotechnical conditions and seismic characteristics. El-Maissi et al. [8] indicated that road networks are critical components of transportation infrastructure, essential for economic and social development, and must maintain functionality during and after seismic events. Recent research has focused on assessing the vulnerability of road networks and their assets, examining damage states and associated impacts. Two main approaches have been employed: physical-based methods, including fragility functions and vulnerability indices, and traffic-based methods, emphasizing accessibility and link importance. This review highlights the strengths and limitations of these methodologies, identifies key research gaps, and provides directions for future studies on seismic resilience of road networks. El-Maissi et al. [9] investigated that urban road networks are key components of resilient infrastructure, requiring robust performance during earthquakes. Previous studies often focused on single-criterion physical vulnerability, neglecting interactions with surrounding built environments. This research introduces an integrated approach using two Vulnerability Indexes: Intrinsic Seismic Vulnerability (ISVI) for direct roadway damage and Eccentric Seismic Vulnerability (ESVI) for impacts from adjacent building damage. The combined assessment enhances emergency planning and accessibility to critical services, providing a comprehensive tool for urban resilience and risk mitigation.

Yildirim et al. [10] indicated that Seismic events pose critical risks to urban road infrastructure, affecting both road networks and adjacent buildings. This study proposes an integrated vulnerability assessment using an Interval-valued Fermatean fuzzy Analytic Hierarchy Process, combining quantitative and qualitative criteria to evaluate risk for each road segment. The methodology captures interactions between damaged buildings, road networks, and disaster response, enhancing preparedness and mitigation strategies. Case studies in Istanbul and Gölbaşı, Türkiye, validate the approach and demonstrate its effectiveness in identifying high-risk areas and supporting resilient urban infrastructure planning. Broniewicz and Ogrodnik [11] reviewed recent literature on multi-criteria decision-making (MCDM/MCDA) in the transport sector, highlighting popular methods and emerging research trends from 2021 to 2024. A case study on a road investment in Poland demonstrates the application of different criteria weighting techniques, including AHP, Fuzzy AHP, and CRITIC. The TOPSIS method was employed to rank project alternatives, with results compared to official design documentation. The findings illustrate the effectiveness of MCDM approaches for transport decision-making and emphasize the influence of weighting methods on project evaluation outcomes.

Overall, the existing body of literature demonstrates significant progress in modeling and assessing the seismic performance of road embankments [12-15]. However, there remains a clear need for comprehensive numerical studies that integrate advanced constitutive models, site-specific soil conditions, groundwater effects, and realistic seismic inputs within a unified framework. Addressing these gaps is essential for improving the reliability of embankment performance predictions and for developing practical design and retrofit strategies tailored to seismically active regions such as Iran. Despite the substantial advances reported in the literature, several critical gaps remain in the seismic assessment of road embankments. Most existing studies focus either on fragility-based evaluations or on advanced constitutive modeling without systematically investigating the combined influence of seismic intensity measures, frequency content, groundwater conditions, and soil improvement strategies within a unified numerical framework. In particular, the coupled effects of groundwater level variations and liquefaction susceptibility on permanent embankment deformations under realistic earthquake records have received limited attention. To address these gaps, the present study employs advanced finite difference modeling to investigate the seismic response of road embankments under both dry and saturated conditions, explicitly accounting for key earthquake characteristics and soil behavior. The novelty of this research lies in the integrated evaluation of embankment deformation mechanisms, liquefaction effects, and stabilization measures, providing design-oriented insights that contribute to the development of more resilient and region-specific seismic design and retrofitting guidelines for transportation infrastructure.

3. Numerical simulation

3.1. Static analysis

The seismic response of the material and its tendency for strain softening are largely governed by its initial stress state and inherent properties [16]. To simulate a steady-state free-field condition, the model is initialized with geostatic stresses assigned to each grid zone, which allows the system to achieve equilibrium through mechanical computations. In the static analysis, the road embankment was subjected exclusively to gravitational loading. The base of the model was fully constrained in all directions, while the lateral boundaries were restricted along the x-axis. It is essential to disable the flow calculation feature during this stage. Moreover, to avoid coupling effects between pore pressure and volumetric deformation, the bulk modulus of water was set to zero.

3.2. Dynamic analysis

Following the static analysis under effective stress conditions, the dynamic response of the embankment system was investigated through the following procedure:

Step 1 – Baseline Correction

Prior to applying the horizontal components of the earthquake records, baseline correction of the acceleration histories was performed. Direct double integration of uncorrected acceleration often results in residual displacements at the end of the motion. To address this, a low-frequency adjustment was added to the input ground motion, ensuring that the final displacement returns to zero.

Step 2 – Wave Propagation Considerations

Accurate wave propagation is critical in dynamic simulations. Errors may arise if the numerical grid does not appropriately capture the highest shear wave frequencies of the soil. The finite difference grid spacing was determined based on the maximum allowable shear wave frequency, f, calculated as [16]:

$$f = \frac{c_s}{10\Delta l} \quad (1)$$

where

c_s is the shear wave velocity of the soil, and Δl represents the largest grid dimension. A uniform grid size of 1 m × 1 m was adopted, resulting in a maximum permissible frequency of 5 Hz corresponding to the slowest soil layers. To ensure numerical stability, the input earthquake records were filtered with a low-pass filter set to 4 Hz, accounting for potential reductions in shear wave velocity due to plastic deformation during seismic loading.

Step 3 – Dynamic Boundary Conditions: Kuhlemeyer RL, Lysmer

To simulate free-field conditions at the model boundaries, free-field boundary conditions were applied laterally, while absorbing boundaries were implemented to emulate the outward propagation of waves at the base. The viscous boundaries developed by Kuhlemeyer Roger and Lysmer [17] were utilized to effectively absorb outgoing waves, thus approximating half-space behavior. The horizontal components of acceleration records from the Imperial Valley, Kobe Port Island, and Kocaeli earthquakes were applied at the model base. These accelerations were converted into equivalent shear stress waves following the procedure described in FLAC [16].

Step 4 – Rayleigh Damping Implementation

Rayleigh damping, comprising two frequency-dependent viscous components, was applied to all model elements. By selecting an appropriate center frequency, damping can be maintained nearly constant across a range of frequencies surrounding this point [16]. The center frequency was chosen between the natural frequency of the system and the predominant frequency of the input motion, and a damping ratio of 5% was assigned. Dynamic simulations were then performed, and the responses were recorded for subsequent interpretation and assessment.

3.3. Equilibrium equations and constitutive model

In more general situations for which the soil is not in static equilibrium, for example, during seismic wave propagation, the governing equations are the equations of motion. The dynamic analyses were conducted as fully non-linear elasto-plastic two-dimensional coupled stress-flow analyses with coupled liquefaction triggering using the Fast Lagrangian Analysis of Continua (*FLAC*) [16]. In *FLAC*, calculation of displacements and pore pressure is carried out by solving a coupled system of equations, including the motion equation and the diffusion equation. In this code, saturated soil is treated as a two-phase material. Biot coupled equations were used for the soil and water phases. Pore pressure generation is incremental and fully integrated with the nonlinear dynamic analyses. During dynamic analyses, pore fluid simply responds to changes in pore volume caused by mechanical dynamic loading. The average pore pressure does not vary significantly during the analysis. It is known, however, that pore pressure may build up considerably during cyclic shear loading. It is important to incorporate this physical process in the coupled nonlinear dynamic analysis. Martin Geoffrey et al. [18] proposed the following empirical equation that relates the increment of volume decrease,$\Delta\varepsilon_{vd}$, to the cyclic shear-strain amplitude,γ:

$$\Delta\varepsilon_{vd} = c_1(\gamma - c_2\varepsilon_{vd}) + \frac{c_2\varepsilon_{vd}^2}{\gamma - c_4\varepsilon_{vd}} \quad (2)$$

Byrne [19] proposed a modified two-parameter effective stress model (Eq. 3).

$$\frac{\Delta\varepsilon_{vd}}{\gamma} = c_1 exp\left(-c_2\left(\frac{\varepsilon_{vd}}{\gamma}\right)\right) \quad (3)$$

Where c_1 and $c_2$are constants with different interpretations from Eq. (3), c_1 can be derived from relative density, D_r, as follows:

$$c_1 = 7600(D_r)^{-2.5} \quad (4)$$

$$c_2 = \frac{0.4}{c_1} \quad (5)$$

Further, Byrne [19] represented an empirical relation between D_r and a normalized standard penetration test $(N_1)_{60}$ values.

$$D_r = 15\ (N_1)_{60}^{0.5} \quad (6)$$

$$c_1 = 8.7\ (N_1)_{60}^{-1.25} \quad (7)$$

The above mentioned formulation is available in FLAC as a built-in model and was adopted in this study along with a bilinear, elastic- perfectly plastic stress–strain relationship and Rayleigh damping. Therefore, during dynamic analysis, as effective stresses decrease with increase in pore pressure, the soil begins to yield and increments of permanent deformation are accumulated.

3.4. Numerical modeling of seismic response of road embankments on liquefiable soils

Numerical analyses of the road embankments were conducted using the finite difference software FLAC [16] to investigate their seismic response on liquefiable soils. The main objective of the simulations was to quantify embankment deformation and stability under dynamic earthquake loading conditions. The embankment was founded on a 10 m thick layer of loose sand with a relative density of 30% (D_r = 30%), modeled as a homogeneous, cohesionless material following the Mohr–Coulomb failure criterion. This liquefiable sand layer was placed atop a dense gravelly stratum representing the underlying foundation soil, based on geotechnical site investigations. To capture realistic pore pressure effects, the water table was gradually raised to exceed the sand layer, ensuring full saturation of the liquefiable soil. The material parameters for both the soils are summarized in Table 1. The numerical model setup allowed for an explicit evaluation of liquefaction-induced settlements, lateral spreading, and potential slope instabilities under prescribed earthquake motions, providing insights into the coupled behavior of embankments and their supporting soils during seismic events.

Table 1. Material properties of the road embankment and foundation soils used in the seismic analysis.

Material type	Υ_{dry} (kg/m^3)	Υ_{sat} (kg/m^3)	φ	C (KPa)	ψ	v	K (m/s)	n	E (KPa)	$N_{1(60)}$
Road embankments	17	19	32	1	2	0.25	1×10^{-3}	0.35	8×10^4	16
Sand	16	18	25	0	0	0.3	1×10^{-6}	0.44	2×10^4	10
Dense gravelly soil	19	21	38	0	8	0.25	1×10^{-7}	0.24	1.2×10^4	45

The finite difference model of the road embankment and underlying soil layers is illustrated in Fig. 8. To represent the seismic response of the liquefiable silt layer, the Finn constitutive model was employed. This model incorporates a coupled effective stress framework, combining the Mohr–Coulomb failure criterion with volumetric strain–based pore water pressure generation, enabling a realistic simulation of liquefaction-induced behavior. Boundary conditions were applied by fully restraining displacements at the base of the model, while the embankment and soil layers were allowed to deform freely elsewhere. Prior to applying dynamic earthquake excitations, the model was brought to static equilibrium to ensure a stable initial stress state. This approach allowed for a robust evaluation of embankment settlements, lateral spreading, and slope stability under seismic loading, capturing the coupled interaction between the embankment and the liquefiable foundation soils.

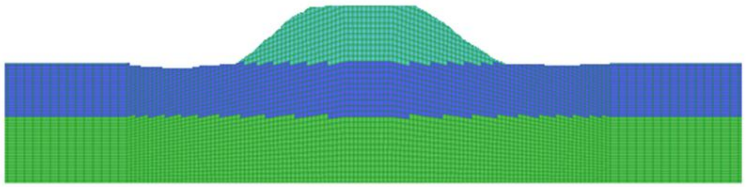

Fig. 8. Schematic geometry and finite difference mesh of the road embankment model used in the seismic analysis.

Each numerical model was subjected to earthquake excitation derived from a scaled record of the Kobe earthquake (1995), Northridge (1994), and Loma Prieta (1989) (Fig. 9). The selected ground motion records were obtained from the PEER Strong Motion Database, as summarized in Table 2. The analyses focused on evaluating the seismic response of the embankments by monitoring the evolution of excess pore water pressure ratios ($r_u = \Delta u/\sigma_0$), as well as horizontal and vertical displacements at the crest and along the slopes. This approach enabled a detailed assessment of embankment deformation mechanisms and liquefaction-induced effects under realistic seismic loading conditions.

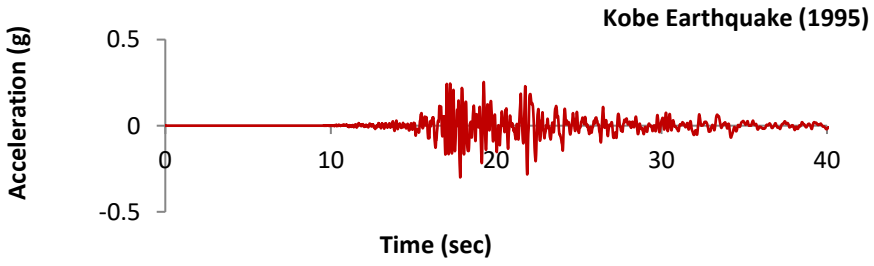

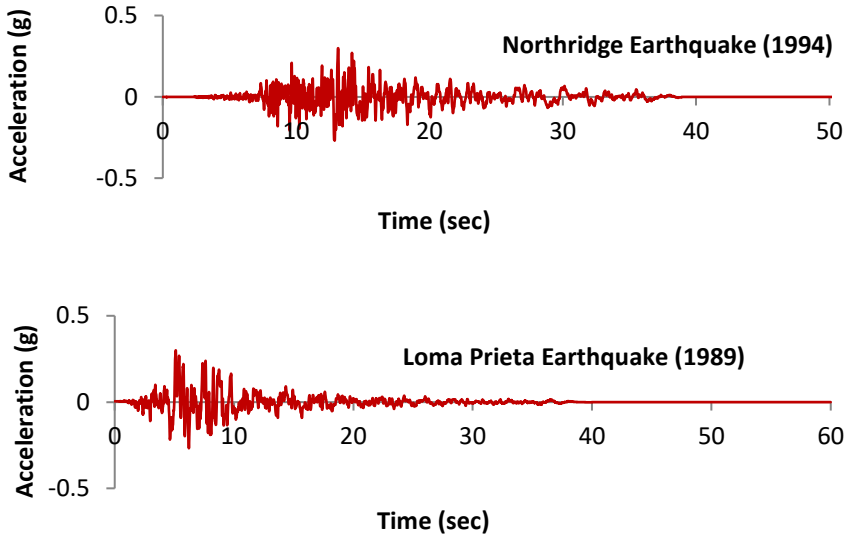

Fig. 9. Ground motion records selected for dynamic time-history analyses of the road embankment models.

Table 2. Seismic input parameters used in the numerical analysis.

Record	M_w	Predominant period, $T_p(s)$	PGA (g)	I_a (m/s)	PGA/PGA (s)	$D_{5-95}(s)$	Specific energy density $(J.m^{-2}sec^{-2})$
Elcentro (1940)	7.2	0.46	0.32	0.392 2.321 5.725	0.097	25	2170.75
Kobe (1995)	6.9	0.16	0.32	0.320 1.896 4.692	0.082	8.7	1256
Kocaeli (1999)	7.4	1.4	0.32	0.232 1.33 3.284	0.182	10	10395

3.5. Model validation

The soil behavior in this study was represented using a combination of the elasto-plastic Mohr–Coulomb model and the Finn constitutive model to capture liquefaction-induced phenomena in loose, saturated granular soils. Material properties, including bulk and shear moduli and soil density, were calibrated based on centrifuge test results to ensure realistic response under dynamic loading. Fully coupled nonlinear dynamic analyses were conducted using the explicit finite difference code FLAC (Itasca) [16], which solves a coupled system of equations encompassing both the equations of motion and pore pressure diffusion. In this framework, saturated soils are modeled as two-phase materials using Biot's theory to account for soil–water interactions. Prior to applying seismic excitation, static analyses were performed under gravity loading with fully fixed base boundaries and lateral boundaries constrained in the horizontal direction. To decouple pore pressure from mechanical volume changes, the water bulk modulus was set to zero. The cyclic pore pressure generation in the liquefiable soil was modeled following the empirical relationship proposed by Byrne [19], based on Martin Geoffrey et al. [18], which links volumetric strain increments to the amplitude of cyclic shear strain. This approach was implemented in FLAC using the built-in model along with a bilinear elastic–perfectly plastic stress–strain response and Rayleigh damping. During dynamic simulations, effective stresses decreased with increasing pore pressure, initiating soil yielding and progressive accumulation of permanent deformations. The model was validated by comparing the evolution of excess pore pressures obtained from numerical analyses with centrifuge experimental measurements (Fig. 10). The close agreement between predicted and observed pore pressure curves confirms the reliability of the numerical approach for simulating liquefaction-induced behavior and supports its application for assessing the seismic performance of road embankments founded on liquefiable soils.

4. Result and discussion

This section presents a detailed evaluation of the dynamic response of the road embankment and the underlying liquefiable soil. The analyses focus on the temporal evolution of excess pore water pressure ratios (r_u), as well as vertical and horizontal deformations, both within the free-field soil and along the embankment. By comparing the time histories at key locations, insights into the mechanisms driving embankment settlements, lateral spreading, and overall stability under seismic loading are obtained. The results are interpreted in the context of the interaction between cyclic shear stresses, pore pressure development, and the mechanical properties of the soil layers. Trends in pore pressure generation and dissipation are correlated with corresponding deformations, highlighting the influence of liquefaction on embankment performance. Furthermore, spatial variations in settlement and lateral displacement are examined to identify critical zones susceptible to instability. This comprehensive analysis provides a mechanistic understanding of the seismic behavior of embankments on liquefiable foundations and informs the effectiveness of

potential mitigation or stabilization strategies.

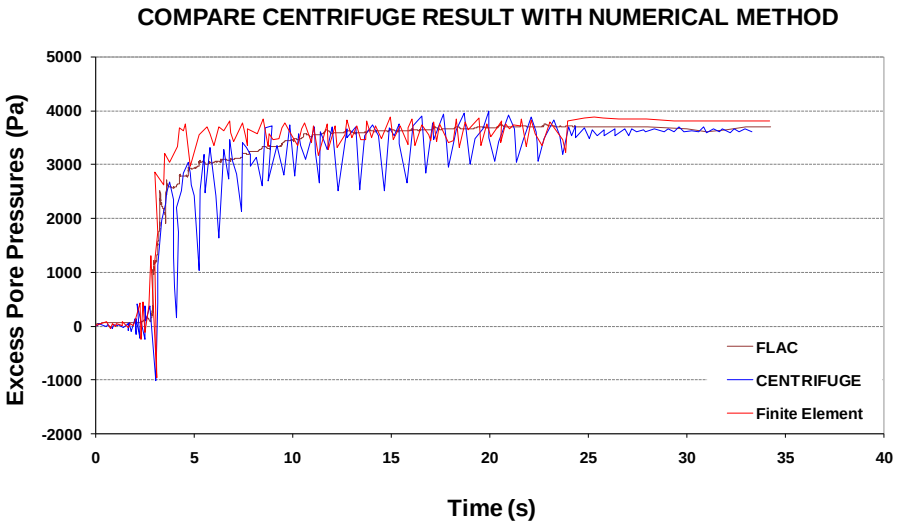

Fig. 10. Comparison of excess pore pressure evolution between centrifuge experiments and the numerical model.

4.1. Free field

The temporal variation of excess pore water pressure ratio (r_u) at different depths in the free-field soil during seismic shaking is presented in Fig. 11. The evolution of r_u is strongly influenced by the characteristics of the earthquake input, with peak values occurring during the maximum strong-motion phase, followed by gradual dissipation. These observations indicate that a substantial portion of the soil experiences a significant reduction in shear strength during the seismic event. The pronounced increase in pore pressure underscores the potential for liquefaction and associated deformations, emphasizing the need for effective mitigation strategies to safeguard the stability and integrity of road embankments constructed on such vulnerable soils.

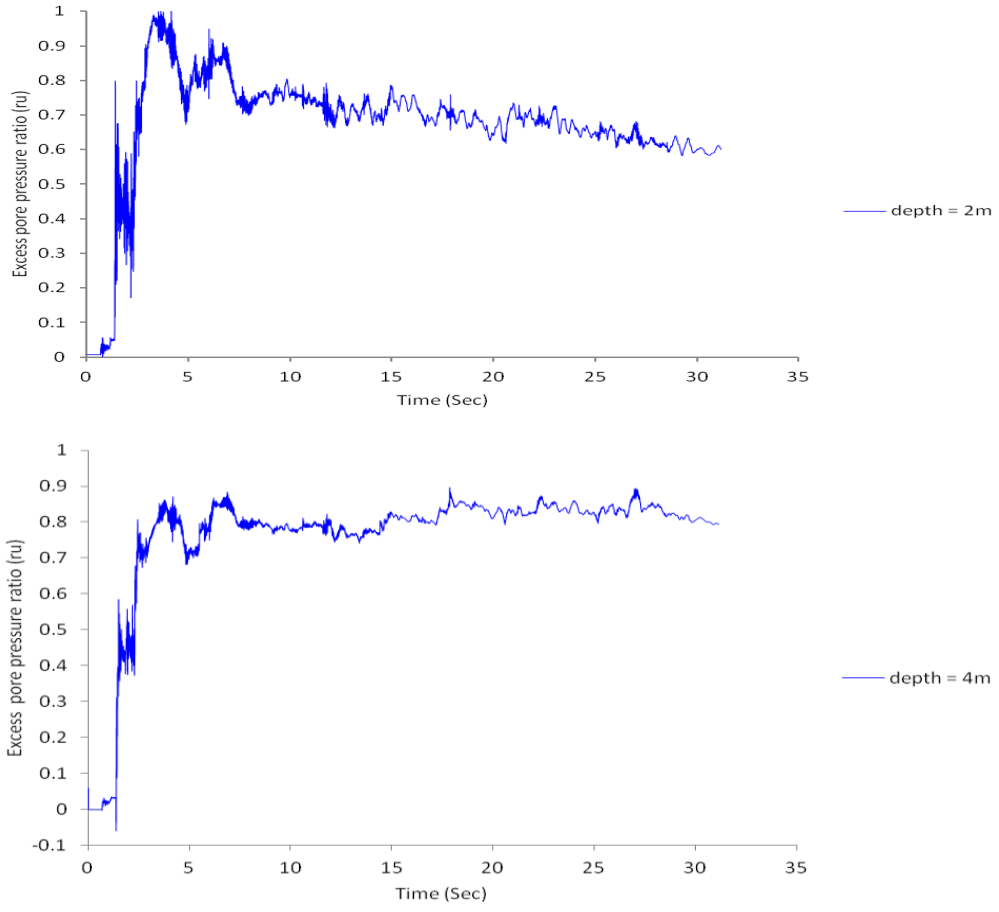

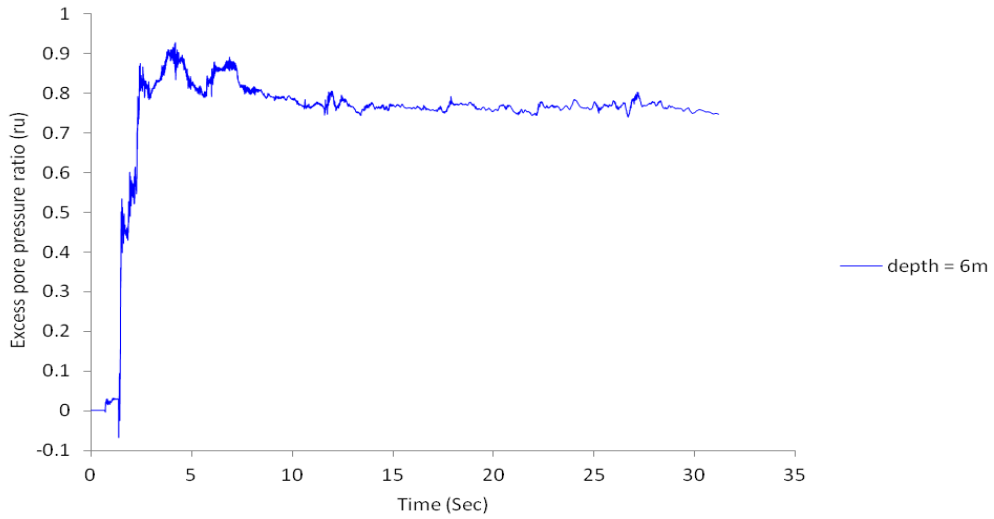

Fig. 11. Evolution of excess pore water pressure ratio at depths of 2, 4, and 6 m in the free-field soil under the Kobe earthquake (0.32 g).

4.2. Conditions of the roadway embankment during seismic loading

The dynamic response of road embankments during strong seismic events, such as the Kobe earthquake, is a critical determinant of transportation infrastructure performance. Under earthquake loading, embankments exhibit vertical settlements driven by soil densification and shear deformation, alongside horizontal displacements caused by reductions in soil shear strength. These deformations can lead to a decrease in embankment height, alterations in slope geometry, surface irregularities, and localized stress concentrations, potentially resulting in partial or localized structural failures. Additionally, asymmetric displacement patterns generate bending and torsional stresses, which further increase the susceptibility of the embankment to cracking and localized deformations (Fig. 12). To mitigate such effects, engineering interventions including dynamic compaction, soil improvement through grouting or chemical stabilizers, enhanced drainage, and resilient design strategies are recommended. The findings underscore the importance of targeted research into embankment stability under seismic excitation, particularly in regions with liquefiable or weak soils, to inform effective design, retrofitting, and risk-reduction strategies.

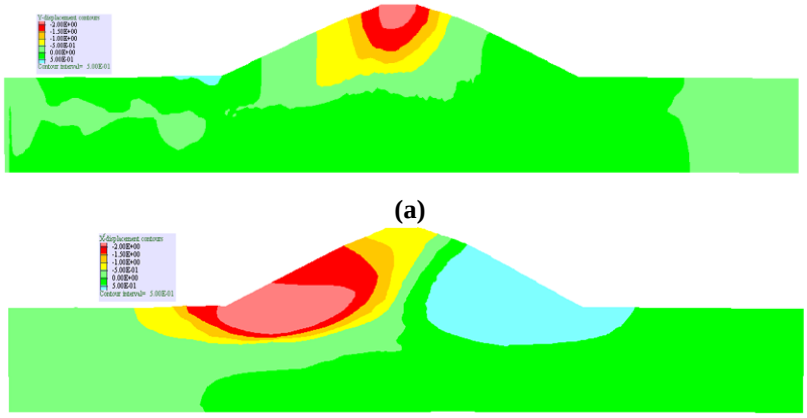

(a)

(b)

Fig. 12. Vertical settlement (a) and horizontal displacement (b) of the road embankment under the Kobe earthquake acceleration record(0.32 g).

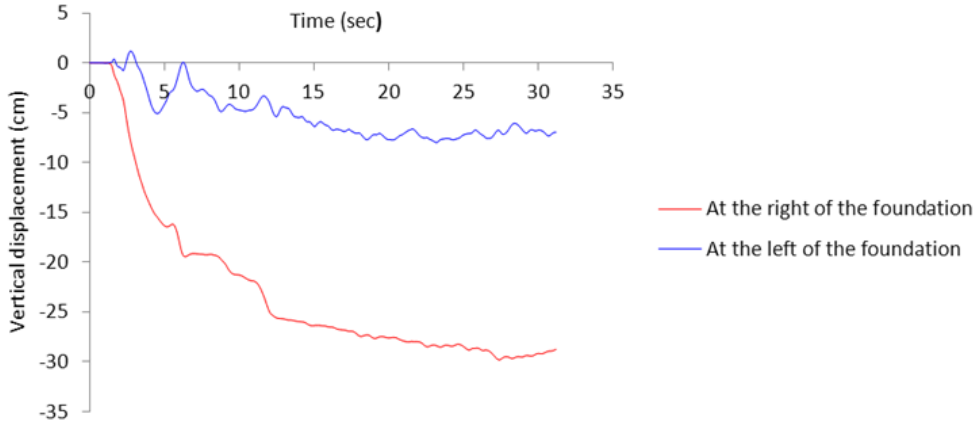

Fig. 13. Vertical settlement profile of the roadway embankment under the Kobe earthquake (0.32 g).

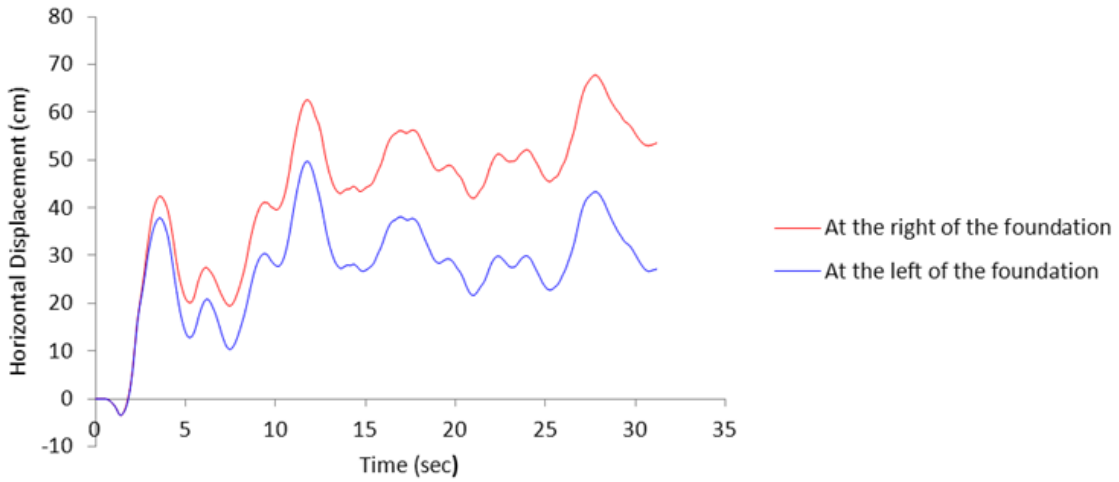

Fig. 14. Lateral displacement profile of the roadway embankment under the Kobe earthquake (0.32 g).

As illustrated in Figs. 13 and 14, the presence of liquefiable soil layers beneath the roadway embankment induces pronounced and non-uniform vertical settlements as well as lateral displacements. Such asymmetric deformations can compromise the structural integrity of the embankment, potentially causing substantial damage to the roadway foundation and affecting its serviceability. These observations highlight the critical influence of underlying soil conditions on seismic performance and underscore the need for targeted mitigation and stabilization measures in embankments constructed on liquefiable deposits.

4.3. Influence of peak ground acceleration (PGA)

The results presented in Tables 3 and 4 indicate that increases in peak ground acceleration (PGA), combined with elevated groundwater levels, substantially amplify both horizontal and vertical deformations of the roadway embankment. Higher PGA intensifies lateral seismic forces, while a raised water table reduces effective soil strength, exacerbating the potential for liquefaction and embankment instability. Under these conditions, the embankment is susceptible to deep surface cracking, localized distortions, and even partial structural failure. To mitigate these risks, strategies such as enhanced drainage systems, soil improvement through grouting or chemical additives, and the design of more resilient embankment structures are recommended. These findings emphasize the critical need for detailed investigations into the combined effects of seismic intensity and hydrogeological conditions on embankment performance. Moreover, they provide a practical basis for developing engineering solutions aimed at improving safety and minimizing earthquake-induced damage to transportation infrastructure.

Table 3. Crest horizontal displacements of the roadway embankment under the Kobe earthquake at varying peak ground accelerations (PGA).

	Horizontal displacement (m)			
Groundwater level from ground surface (cm)	**(PGA = 0.15)**	**(PGA = 0.25)**	**(PGA = 0.35)**	**(PGA = 0.45)**
100	1.32	1.82	2.14	3.62
60	1.86	2.41	3.12	4.15
20	2.52	3.26	3.88	4.65

Table 4. Crest vertical settlements of the roadway embankment under the Kobe earthquake at varying peak ground accelerations (PGA).

	Settlement (m)			
Groundwater level from ground surface (cm)	**(PGA = 0.15)**	**(PGA = 0.25)**	**(PGA = 0.35)**	**(PGA = 0.45)**
100	1.45	1.75	2.35	3.11
60	1.84	2.15	2.85	3.57
20	2.12	2.46	3.42	4.86

4.4. Influence of thickness of liquefiable soil

It is shown (in Fig. 15) that the effect of thickness of liquefiable soil on horizontal and vertical displacement profile of the roadway embankment under the different earthquakes. It is clear that the amount of horizontal and vertical displacement significantly increase with increase of thickness of liquefiable soil. This rate in higher PGA is more obvious especially (PGA > 0.35 g).

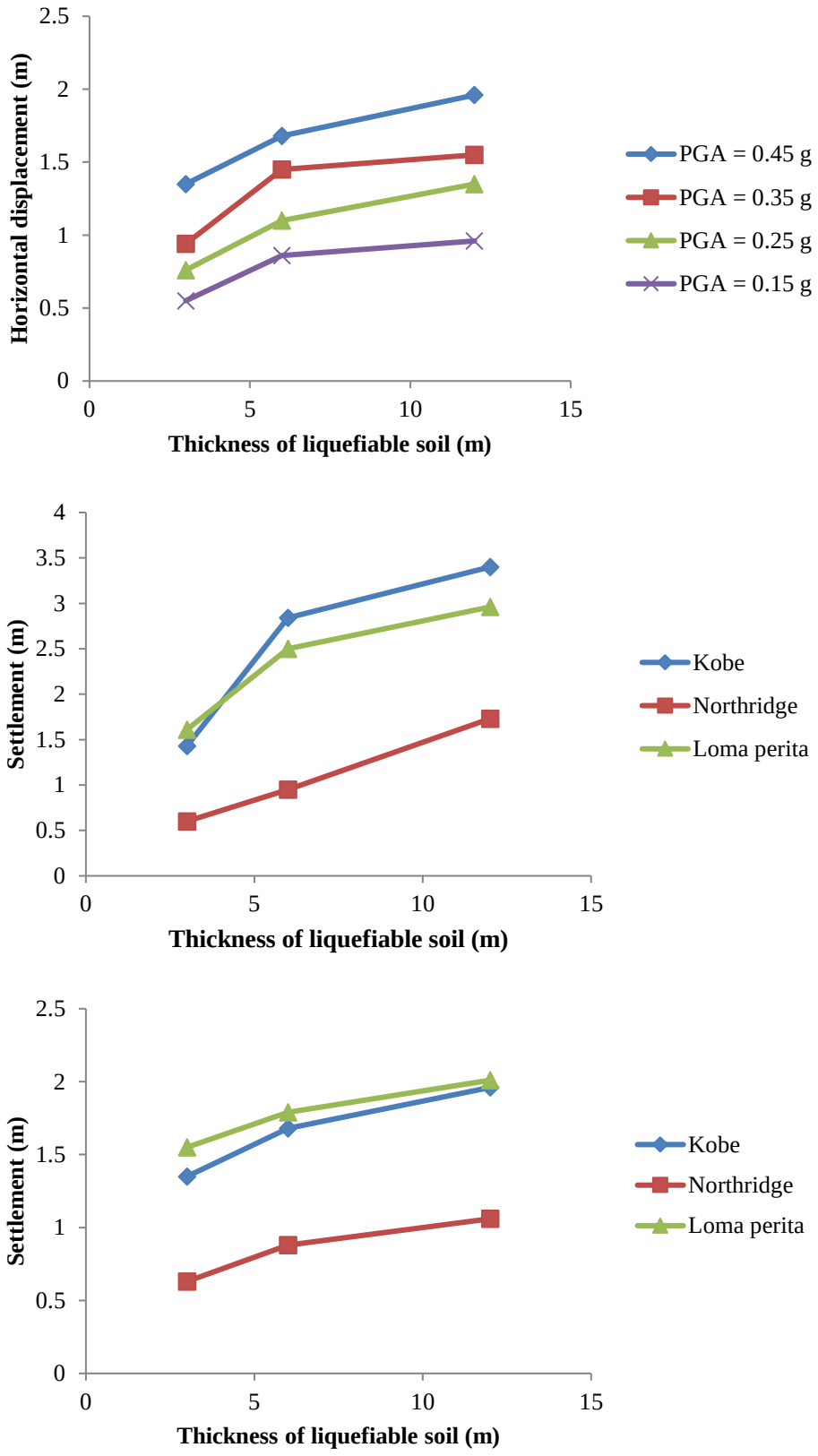

Fig. 15. Horizontal and vertical displacement profile of the roadway embankment under the different earthquakes.

5. Conclusion

This study employed numerical simulations to investigate the seismic response of road embankments constructed on liquefiable soils. The results demonstrate that the frequency content of earthquake input is a key parameter influencing both vertical and horizontal deformations. Even under similar peak ground accelerations, differences in seismic energy distribution can result in substantial variations in settlement and lateral displacement, highlighting the necessity of accounting for both PGA and input energy characteristics in seismic assessments. The analyses further indicate that increases in ground acceleration and elevated groundwater levels significantly exacerbate embankment deformations. Higher seismic forces, combined with reduced effective soil strength due to increased pore water pressure, amplify the risk of liquefaction and slope instability. Free-field analyses revealed that lateral

displacements, particularly near the surface, contribute notably to embankment instability. Peak settlements were observed predominantly during the strong-motion phase, often resulting in deep cracking, localized distortions, reductions in embankment height, and changes in surface slope. These deformations can compromise the structural integrity of the embankment and adversely affect the performance of adjacent transportation infrastructure. The findings emphasize the importance of comprehensive seismic evaluations for road embankments, particularly in regions with liquefiable soils. Mitigation strategies such as enhanced drainage to control pore pressure, soil improvement through grouting or dynamic compaction, and resilient structural design capable of accommodating a wide range of seismic frequencies and intensities are critical for reducing damage and improving overall stability. Implementing these measures not only protects the embankment but also contributes to the resilience and safety of transportation networks in seismically active areas.

Statements & Declarations

Author contributions

Vahid Sadeghi: Investigation, Formal analysis, Data curation, Software, Writing - Original Draft.

Mohsen Bagheri: Project administration, Resources, Software, Writing - Review & Editing.

Jaber Abasi Hamidi: Conceptualization, Methodology, Software, Writing - Review & Editing.

Funding

The authors received no financial support for the research, authorship, and/or publication of this article.

Data availability

The data presented in this study will be available on interested request from the corresponding author.

Declarations

The authors declare no conflict of interest.

References

[1] Argyroudis, S., Kaynia, A. M. Analytical seismic fragility functions for highway and railway embankments and cuts. Earthquake Engineering & Structural Dynamics, 2015; 44: 1863–1879. doi:10.1002/eqe.2563.

[2] Argyroudis, S., Kaynia, A. M., Pitilakis, K. Development of fragility functions for geotechnical constructions: Application to cantilever retaining walls. Soil dynamics and earthquake engineering, 2013; 50: 106–116. doi:10.1016/j.soildyn.2013.02.014.

[3] Ledezma, C., Hutchinson, T., Ashford, S. A., Moss, R., Arduino, P., Bray, J. D., Olson, S., Hashash, Y. M., Verdugo, R., Frost, D. Effects of ground failure on bridges, roads, and railroads. Earthquake Spectra, 2012; 28: 119–143. doi:10.1193/1.4000024.

[4] Cubrinovski, M., Robinson, K., Taylor, M., Hughes, M., Orense, R. Lateral spreading and its impacts in urban areas in the 2010–2011 Christchurch earthquakes. New Zealand Journal of Geology and Geophysics, 2012; 55: 255–269. doi:10.1080/00288306.2012.699895.

[5] Khalil, C., Rapti, I., Lopez-Caballero, F. Numerical Evaluation of Fragility Curves for Earthquake-Liquefaction-Induced Settlements of an Embankment. 1st ed. Reston (VR): American Society of Civil Engineers (ASCE); 2017. doi:10.1061/9780784480700.

[6] Oblak, A., Kosič, M., Viana Da Fonseca, A., Logar, J. Fragility Assessment of Traffic Embankments Exposed to Earthquake-Induced Liquefaction. Applied Sciences, 2020; 10: 6832. doi:10.3390/app10196832.

[7] Chakraborty, A., Sawant, V. A. Calibration of UBC3D-PLM Constitutive Model to Simulate the Dynamic Response of Earthen Embankment Resting on Liquefiable Soil. In: Proceedings of 17th Symposium on Earthquake Engineering (Vol. 3); 2023; Singapore. p. 771–783.

[8] El-Maissi, A. M., Argyroudis, S. A., Nazri, F. M. Seismic Vulnerability Assessment Methodologies for Roadway Assets and Networks: A State-of-the-Art Review. Sustainability, 2021; 13: 61. doi:10.3390/su13010061.

[9] El-Maissi, A. M., Argyroudis, S. A., Kassem, M. M., Mohamed Nazri, F. Integrated seismic vulnerability assessment of road network in complex built environment toward more resilient cities. Sustainable Cities and Society, 2023; 89: 104363. doi:10.1016/j.scs.2022.104363.

[10] Yildirim, A. K., Kavus, B. Y., Karaca, T. K., Bozbey, İ., Taskin, A. A novel seismic vulnerability assessment for the urban roadway by using interval valued fermatean fuzzy analytical hierarchy process. Natural Hazards, 2024; 120: 13811–13834. doi:10.1007/s11069-024-06748-1.

[11] Broniewicz, E., Ogrodnik, K. Application Potential of MCDM/MCDA Methods in Transport—Literature Review and Case Study. Sustainability, 2025; 17: 7671. doi:10.3390/su17177671.

[12] Maruyama, Y., Lai, S., Lchii, K., Tobita, T. Fragility functions for highway embankments based on damage data from recent earthquakes in Japan. Soil dynamics and earthquake engineering, 2010; 30: 1158–1167. doi:10.1016/j.soildyn.2010.04.013.

[13] Yang, M., Taiebat, M., Dafalias, Y. F. SANISAND-MSf: a sand plasticity model with memory surface and semifluidised state. Geotechnique, 2022; 72: 227–246. doi:10.1680/jgeot.19.P.363.

[14] López-Querol, S., Blázquez, R. Identification of failure mechanisms of road embankments due to liquefaction: optimal corrective measures at seismic sites. Canadian Geotechnical Journal, 2006; 43: 889–902. doi:10.1139/t06-051.

[15] Soleimanian, N., Akhtarpour, A., Baradaran, M. S. Experimental and Numerical Investigation of Landfill Leachate Emission in Unsaturated Sandy Soils. Civil Engineering and Applied Solutions, 2026; 2: 58–73. doi:10.22080/ceas.2025.29684.1028.

[16] Itasca, F. FLAC (Fast Lagrangian Analysis of Continua)-Fast Lagrangian Analysis of Continua. User Manual, Itasca Consulting Group, 2011;

[17] Kuhlemeyer Roger, L., Lysmer, J. Finite Element Method Accuracy for Wave Propagation Problems. Journal of the Soil Mechanics and Foundations Division, 1973; 99: 421–427. doi:10.1061/JSFEAQ.0001885.

[18] Martin Geoffrey, R., Seed, H. B., Finn, W. D. L. Fundamentals of Liquefaction under Cyclic Loading. Journal of the Geotechnical Engineering Division, 1975; 101: 423–438. doi:10.1061/AJGEB6.0000164.

[19] Byrne, P. M. A Cyclic Shear-Volume Coupling and Pore Pressure Model for Sand. In: InternationalConferences on Recent Advances in Geotechnical Earthquake Engineering and Soil Dynamics; 1991 Mar 12–13; St. Louis, Missouri. p. 47–55.